Testing tripartite Mermin inequalities by spectral joint measurements of qubits

J. S. Huang, C. H. Oh, and L. F. Wei

Phys. Rev. A **83**, 062108 — Published 13 June 2011

DOI: 10.1103/PhysRevA.83.062108

Testing tripartite Mermin inequalities by spectral joint-measurements of qubits

J. S. Huang,[1,2] C. H. Oh*,[2] and L. F. Wei†[1,3]

[1]*Quantum Optoelectronics Laboratory, School of Physics and Technology, Southwest Jiaotong University, Chengdu 610031, China*

[2]*Centre for Quantum Technologies and Department of Physics, National University of Singapore, 3 Science Drive 2, Singapore 117542, Singapore*

[3]*State Key Laboratory of Optoelectronic Materials and Technologies, School of Physics and Engineering, Sun Yat-Sen University Guangzhou 510275, China*

Abstract

Using spectral joint-measurements of the qubits, we propose a scheme to test the tripartite Mermin inequality with three qubits dispersively-coupled to a driven cavity. First, we show how to generate a three-qubit Greenberger-Horne-Zeilinger (GHZ) state by only one-step quantum operation. Then, spectral joint-measurements are introduced to directly confirm such tripartite entanglement. Assisted by a series of single-qubit operations, these measurements are further utilized to test the Mermin inequality. The feasibility of the proposal is robustly demonstrated by the present numerical experiments.

PACS number(s): 03.65.Ud, 42.50.Dv, 42.50.Pq

* phyohch@nus.edu.sg

† weilianfu@gmail.com

I. INTRODUCTION

Entanglement [1] is at the heart of the quantum theory and also the crucial resource of quantum information processing [2, 3]. It is one of the most important ingredients of various intriguing phenomena, e.g., quantum teleportation [4, 5], secret sharing [6], and remote state preparation [7], etc. Therefore, generating and verifying the existence of entanglement are of great importance.

Since Bell inequality [8] and its CHSH version [9] was formulated to test the correlations between two particles, numerous experiments with bipartite entanglement, e.g., photons [10], trapped ions [11, 12], neutrons [13] and Josepson junctions [14, 15], etc., have been demonstrated to probe the nonlocal nature of quantum mechanics. As all these experiments support quantum mechanics and rule out the local hidden-variable theories, Bell inequality can be served as an important witness of quantum entanglement.

With the developments of quantum technology, entanglement shared by multiple particles plays more and more important roles for large-scale quantum information processing and many-body quantum mechanics. Multipartite entangled states have been demonstrated with atoms [16, 17], photons [18–21], trapped ions [22–24], and also Josephson junction circuits [25, 26], etc. Basically, multipartite entanglement can be robustly verified by the standard quantum-state tomographic technique, i.e., reconstructing their density matrixes by a series of quantum measurements. Instead, one can also verify entanglement by testing the violation of the multipartite Bell-type inequality, such as Mermin inequality [27]:

$$Q = |E(\theta_1', \theta_2, \theta_3) + E(\theta_1, \theta_2', \theta_3) + E(\theta_1, \theta_2, \theta_3') - E(\theta_1', \theta_2', \theta_3')| \leq 2. \tag{1}$$

with three-qubit systems. Indeed, the violation of this inequality has been experimentally demonstrated with three-photon entanglement [19, 20]. In the Eq. (1) above, $\{\theta_1, \theta_2, \theta_3, \theta_1', \theta_2', \theta_3'\}$ are the set of controllable local-variables of the three independent particles, and the correlation function $E(\theta_1, \theta_2, \theta_3)$ is the ensemble average over the measurement outcomes for the local settings: $\theta_1, \theta_2, \theta_3$.

As a possible experimental demonstration, in this paper we discuss how to perform the test of a tripartite Mermin inequality with three qubits coupled to a driven cavity. Three-qubit Greenberger-Horne-Zeilinger (GHZ) [28] entangled state is the starting point of our test. Note that an efficient approach to prepare multipartite GHZ entanglement, assisted by a quantized cavity, has been proposed in Ref. [16]. In the scheme of Ref. [16], a series of atoms are sequentially passed through

the cavity, and their interactions with the cavity can be controlled by adjusting their flying times. As a consequence, GHZ-entanglement between the atoms can be produced, and the cavity mode is left in its vacuum state. Differing from Ref. [16], here we discuss how to prepare the atomic qubits contained in a common cavity, where the atomic qubits interact simultaneously with the cavity mode. By appropriately driving the cavity, e.g., tuning the driving time, the atomic qubits and the cavity mode can be decoupled from each other at certain instants of time, and consequently the desired GHZ entanglement between the atomic qubits is generated. Two main aspects in the present proposal are: (i) an one-step approach is proposed to generate the desired GHZ state, and (ii) a spectral measurement method is introduced to implement the joint measurements of these three qubits to test the Mermin inequality. In principle, our proposal could be further generalized to the cases with more than three particles. The paper is organized as: In Sec. II, we briefly describe how to generate the tripartite GHZ entangled state of three qubits coupled dispersively to a driven cavity. Then, by introducing a spectral joint-measurement method via detecting the photon transmission through the driven cavity, we propose a simple two-step method to confirm such a tripartite GHZ entanglement. In Sec. III, we propose a scheme on how to encode various local variables into the prepared GHZ entanglement via performing suitable single-qubit operations, and implement the test of the Mermin inequality by the introduced joint-measurements. Discussions on the feasibility of our proposal are given in Sec. IV.

II. GENERATION AND CONFIRMATION OF THE GHZ STATE OF QUBITS COUPLED TO A DRIVEN CAVITY-QED SYSTEM

A. Preparation of tripartite GHZ state by only one-step quantum operation

We consider a driven cavity-qubit system, wherein three qubits without interbit interaction are respectively coupled to a common cavity mode. Such a cavity-qubit system can be described by the Tavis-Cummings Hamiltonian [29] ($\hbar = 1$ throughout the paper)

$$H_{\rm TC} = \omega_r \hat{a}^\dagger \hat{a} + \sum_{j=1,2,3} [\frac{\omega_j}{2}\sigma_{z_j} + g_j(a^\dagger \sigma_{-_j} + a\sigma_{+_j})], \tag{2}$$

where $a^{(\dagger)}$ and $\sigma_{\pm_j}$ are the ladder operators for the photon field and the jth qubit, respectively; ω_r is the cavity frequency, ω_j the jth qubit transition frequency, and g_j the coupling strength between

the jth qubit and the cavity. The driving of the cavity can be modeled by

$$H_d = \varepsilon(a^\dagger e^{-i\omega_d t} + a e^{i\omega_d t}), \tag{3}$$

where ε is the amplitude and ω_d the frequency of the external drive.

Following Ref. [30], after a displacement transformation $D(\alpha) = \exp(\alpha\hat{a}^\dagger - \alpha^*\hat{a})$, the displaced Hamiltonian of the composite system reads

$$\begin{aligned} H_{\rm T} &= D^\dagger(\alpha)(H_{\rm TC} + H_d)D(\alpha) - iD^\dagger(\alpha)\dot{D}(\alpha) \\ &= \omega_r a^\dagger a + \sum_{j=1,2,3}[\frac{\omega_j}{2}\sigma_{z_j} + g_j(a^\dagger\sigma_{-_j} + a\sigma_{+_j}) + g_j(\alpha^*\sigma_{-_j} + \alpha\sigma_{+_j})]. \end{aligned} \tag{4}$$

Now, we let $\omega_d = \omega_j$, $\dot{\alpha} = -i\omega_r\alpha - i\varepsilon\exp(-i\omega_d t)$, and work in a rotating frame defined by $U_1 = \exp[-it(\omega_r a^\dagger a + \sum\limits_{j=1,2,3}\omega_d\sigma_{z_j}/2)]$, the effective Hamiltonian of the cavity-qubit system takes the form

$$\tilde{H}_{\rm T} = \sum_{j=1,2,3}[\Omega_j\sigma_{x_j} + g_j(a^\dagger\sigma_{-_j}\exp(-i\delta t) + a\sigma_{+_j}\exp(i\delta t))], \tag{5}$$

with the qubit-drive detuning $\delta = \omega_d - \omega_r$ and the Rabi frequency $\Omega_j = \varepsilon g_j/\delta$. Changing to the orthogonal bases $|\pm_j\rangle = (|1_j\rangle \pm |0_j\rangle)/\sqrt{2}$, and in the interaction picture, we get

$$\begin{aligned} H_I = &\sum_{j=1,2,3}\frac{g_j}{2}a^\dagger\exp(-i\delta t)\,[|+_j\rangle\langle+_j| - |-_j\rangle\langle-_j| \\ &+ \exp(i2\Omega_j t)|+_j\rangle\langle-_j| - \exp(-i2\Omega_j t)|-_j\rangle\langle+_j|] + h.c., \end{aligned} \tag{6}$$

where $|\pm_j\rangle$ are the eigenstates of operator σ_{x_j} with eigenvalues ±1. In the strong driving regime: $\Omega \gg \delta, g$, we can eliminate the fast-oscillating terms in Eq. (6) and then have [31, 33]

$$H_I = \sum_{j=1,2,3}\frac{g_j}{2}\sigma_{x_j}[a^\dagger\exp(-i\delta t) + a\exp(i\delta t)]. \tag{7}$$

Note that the operator set $\{\sigma_{x_j}\sigma_{x_{j'}}, a^\dagger\sigma_{x_j}, a\sigma_{x_j}, 1\}$ $(j, j' = 1, 2, 3,$ and $j \neq j')$ form a closed Lie algebra, the time evolution operator related to the above Hamiltonian can be formally written as [32]

$$U_I(t) = \exp[-iC(t)]\prod_j\exp[-i(B_j(t)a\sigma_{x_j} + B_j^*(t)a^\dagger\sigma_{x_j})] \times \prod_{j\neq j'}\exp[-iA_{jj'}(t)\sigma_{x_j}\sigma_{x_{j'}}], \tag{8}$$

with the parameters determined by

$$A_{jj'}(t) = \frac{g_j g_{j'}}{4\delta}[\frac{1}{i\delta}(\exp(-i\delta t) - 1) + t],$$
$$B_j(t) = \frac{g_j}{i2\delta}[\exp(i\delta t) - 1],$$
$$C(t) = \sum_j \frac{g_j^2}{4\delta}[\frac{1}{i\delta}(\exp(-i\delta t) - 1) + t], \quad (9)$$

and $A_{jj'}(0) = B_j(0) = C(0) = 0$.

Suppose that all the qubit-cavity couplings are homogeneous, i.e., $g_j = g$ (for $j = 1, 2, 3$) and set $\delta t = 2n\pi$ for integer n, we have $B(t) = B^*(t) = 0$. Then, the time evolution operator reduces to a simple form

$$U_I(t) = \exp(-i\frac{g^2}{\delta}tS_x^2), \quad (10)$$

with $S_x = \sum_{j=1}^3 \sigma_{x_j}/2$. Return to the Schröinger picture,

$$\begin{aligned} U_S(t) &= U_0(t)U_I(t) \\ &= \exp(-i\omega a^\dagger a t)\prod_j \exp(-i\Omega_j \sigma_{x_j} t)U_I(t) \\ &= \exp(-i\omega a^\dagger a t)\exp(-i2\Omega S_x t - i\frac{g^2}{\delta}tS_x^2). \end{aligned} \quad (11)$$

Here $\Omega_j = \Omega$ for $g_j = g$ mentioned above. Note that the effective coupling S_x^2 can be utilized to directly realize the multi-qubit GHZ state, when the relevant parameters are appropriately chosen [34]. Assume that the three-qubit register is initially at the state

$$|\psi(0)\rangle = |000\rangle, \quad (12)$$

where $|0\rangle$ ($|1\rangle$) denotes the eigenstate of σ_z, $\sigma_z|0\rangle = -1$ ($\sigma_z|1\rangle = 1$). Using the spin representation of atomic states for the operator $S_z = \sum_{j=1}^3 \sigma_{z_j}/2$, the three-qubit states $|000\rangle$ and $|111\rangle$ can be expressed as collective states $|3/2, -3/2\rangle$ and $|3/2, 3/2\rangle$, respectively. Here, $|J = 3/2, M\rangle$ is the eigenstate of the operators S_z with the eigenvalue M, $M = -J, ..., J$. In terms of the eigenstates of S_x [34], we have

$$|3/2, -3/2\rangle = \sum_{M=-3/2}^{3/2} c_M |3/2, M\rangle_x, \quad (13)$$

and

$$|3/2, 3/2\rangle = \sum_{M=-3/2}^{3/2} c_M (-1)^{3/2-M} |3/2, M\rangle_x, \quad (14)$$

where $M = M' + 1/2$, and M' is an integer. As a consequence, the evolution of the system can be conveniently expressed as (up to a global phase factor)

$$\begin{aligned} |\psi(t)\rangle &= U_S(t)|\psi(0)\rangle \\ &= \sum_{M=-3/2}^{3/2} c_M \exp\left[-i2\Omega t M - i\frac{g^2}{\delta} t M^2\right]|3/2, M\rangle_x \\ &= \frac{1}{\sqrt{2}}(|3/2,-3/2\rangle + i|3/2,3/2\rangle), \end{aligned} \tag{15}$$

with the choice $g^2 t/\delta = (4k+1)\pi/2$ and $\Omega t = (2m + 3/4)\pi$ (k, m are integers). Obviously, at $t = T_n$ the desired GHZ state [33–35]

$$|\psi(T_n)\rangle = U_S(T_n)|\psi(0)\rangle = \frac{1}{\sqrt{2}}(|000\rangle + i|111\rangle) \tag{16}$$

is obtained. In the above, the relations of the integers k, m and n are given by

$$n = \frac{\delta^2}{g^2}k + \frac{\delta^2}{4g^2},\ n = \frac{2\delta^2}{\varepsilon g}m + \frac{3\delta^2}{4\varepsilon g}. \tag{17}$$

B. Confirming the existence of the GHZ entanglement

The GHZ state prepared above by one-step operation can be robustly confirmed by using the standard quantum state tomography, i.e., reconstructing its density matrix. Such an approach was usually utilized to confirm the quantum state in trapped-ions [36], linear optics [19–21] and the solid-state qubits [37–39], etc. However, these confirmations require many kinds of *single-basis* projective measurements assisted by a series of quantum operations, and thus $2^N - 1$ kinds of projections are needed for reconstructing a $N \times N$-matrix, in principle.

Fortunately, a significantly simple approach, i.e., spectral joint-measurements of the qubits [40, 41], can be utilized to high-effectively implement the desired confirmation. By this means the states of the qubits can be jointly detected by probing the steady-state transmission spectra of the driven cavity, which is commonly coupled to the qubits. For the present case, the qubit-cavity detuning $\Delta_j = \omega_j - \omega_r$ is assumed to be much larger than the coupling g, i.e., the system works in the dispersive regime, and the qubit-cavity couplings take the form $H_c = a^\dagger a \sum_{j=1}^3 \Gamma_j \sigma_{z_j}$. This indicates that the qubits cause the state-dependent frequency shift of the cavity. For example, if the qubits is prepared at the joint eigenstate $|000\rangle$ (or $|111\rangle$) of the three qubits, then the frequency of the cavity is shifted as $-\sum_{j=1}^3 \Gamma_j$ (or $\sum_{j=1}^3 \Gamma_j$), which is dependent on the *joint* eigenstate

of the qubits. Thus the steady-state transmission spectra through the driven cavity can mark all the possible joint eigenstates of the qubits. Generally, unknown qubits should be denoted as a superposition of all the possible joint eigenstates of the qubits. As a consequence, the measured transmission spectra $\langle a^{\dagger}a(\omega_d)\rangle_{\rm ss}$ of the driven cavity may appear multiple peaks versus the driving frequency ω_d (see the Appendix for the detailed derivation); each peak marks one of the possible joint eigenstates of the qubits, and its relative height corresponds to the probability of this state superposed in the unknown three-qubit state.

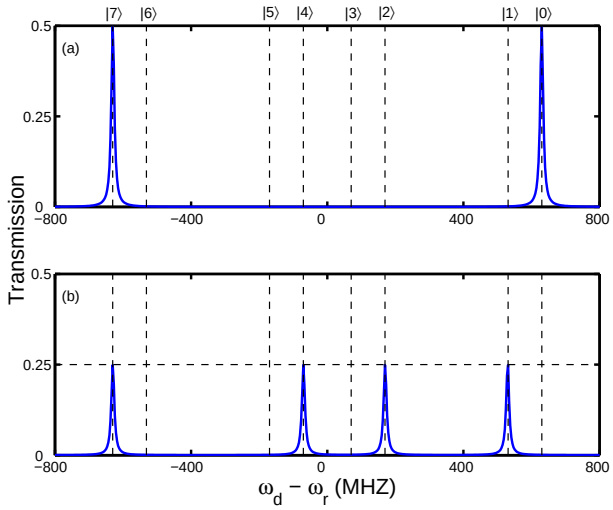

FIG. 1: (Color online) Two spectral joint-measurements to confirm the GHZ entanglement: (a) directly for the GHZ state: $(|000\rangle + |111\rangle)/\sqrt{2}$, and (b) for the state $(|000\rangle + |011\rangle + |101\rangle + |110\rangle)/2$ generated after performing unitary operations on the GHZ state. Here, the parameters are selected as $(\Gamma_1, \Gamma_2, \Gamma_3, \kappa) = 2\pi \times (50, 230, 350, 1.69)$MHz, and $|0\rangle = |000\rangle, |1\rangle = |001\rangle, |2\rangle = |010\rangle, |3\rangle = |011\rangle, |4\rangle = |100\rangle, |5\rangle = |101\rangle, |6\rangle = |110\rangle$, and $|7\rangle = |111\rangle$, respectively.

Specifically, for the GHZ state prepared above the steady-state transmission spectra of the driven cavity should reveal a two-peak structure, see, e.g., Fig. 1(a) with the typical parameters: $(\Gamma_1, \Gamma_2, \Gamma_3, \kappa) = 2\pi \times (50, 230, 350, 1.69)$MHz. To show clearly the simulated results for the test, the parameters Γ_j could be adjusted by adiabatically tuning the qubit-transition frequencies. Desirably, the frequency-shift locations: $-\Gamma_1 - \Gamma_2 - \Gamma_3$, $\Gamma_1 + \Gamma_2 + \Gamma_3$ and the relative heights of these two peaks: 0.5, 0.5, indicate that two joint eigenstates, $|000\rangle$ and $|111\rangle$, are superposed in the measured state with the same superposition probability 0.5. Of course, such a spectral joint-measurement result is just a necessary but not sufficient condition to assure the desired GHZ state, since a statistical mixture of these two joint eigenstates may also yield the same spectral

distributions. To confirm the state $|\psi_{\rm GHZ}\rangle$ is indeed the coherent superposition of the states $|000\rangle$ and $|111\rangle$, we need another spectral joint-measurement by using the quantum coherent effect. This can be achieved by first applying the unitary operation $\prod_{j=1}^{3} R_{x_j}(\pi/4) = \prod_{j=1}^{3} \exp\left(i\pi\sigma_{x_j}/4\right)$ to each qubit to yield the evolution

$$\begin{aligned} |\psi_{\rm GHZ}\rangle \ &\rightarrow \ |\psi'_{\rm GHZ}\rangle = R_{x_1}(\frac{\pi}{4})R_{x_2}(\frac{\pi}{4})R_{x_3}(\frac{\pi}{4})|\psi_{\rm GHZ}\rangle \\ &= \ \frac{1}{2}(|000\rangle - |011\rangle - |101\rangle - |110\rangle), \end{aligned} \tag{18}$$

and then performing the spectral joint-measurement. It is expected that four peaks with the same relative height 0.25 should be observed (see, e.g., Fig. 1(b)), if the prepared state is nothing but the desired tripartite GHZ state. However, if the prepared state is a mixture of the joint eignestates $|000\rangle$ and $|111\rangle$, then eight peaks would be observed.

III. TESTING TRIPARTITE MERMIN INEQUALITY BY SPECTRAL JOINT-MEASUREMENTS

With the prepared GHZ state, we now discuss how to test the tripartite Mermin inequality (1) by jointly measuring the three qubits coupled to the driven cavity. The test includes the following two steps.

First, local parameters $\theta_j (j = 1, 2, 3)$ are encoded into the generated GHZ state (16) by performing the single-qubit Hadamard-like operations

$$\begin{aligned} R_j(\theta_j) \ &= \ R_{z_j}(\theta_j/2)R_{x_j}(\pi/4)R_{z_j}(-\theta_j/2) \\ &= \ \frac{1}{\sqrt{2}} \begin{pmatrix} 1 & ie^{i\theta_j} \\ ie^{-i\theta_j} & 1 \end{pmatrix}. \end{aligned} \tag{19}$$

Here, the typical single-qubit gates $R_{z_j}(\theta) = \exp\left(i\sigma_{z_j}\theta\right)$ and $R_{x_j}(\theta) = \exp\left(i\sigma_{x_j}\theta\right)$ can be easily implemented, see e.g. [30, 41]. After these encoding operations, the generated GHZ state $|\psi_{\rm GHZ}\rangle$ is changed as

$$\begin{aligned} |\psi''_{\rm GHZ}\rangle \ &= \ R_1(\theta_1)R_2(\theta_2)R_3(\theta_3)|\psi_{\rm GHZ}\rangle \\ &= \ \frac{1}{4}[(1 + e^{i(\theta_1+\theta_2+\theta_3)})|000\rangle + (ie^{-i\theta_3} - ie^{i(\theta_1+\theta_2)})|001\rangle + (ie^{-i\theta_2} - ie^{i(\theta_1+\theta_3)})|010\rangle \\ &\quad +(-e^{-i(\theta_2+\theta_3)} - e^{i\theta_1})|011\rangle + (ie^{-i\theta_1} - ie^{i(\theta_2+\theta_3)})|100\rangle + (-e^{-i(\theta_1+\theta_3)} - e^{i\theta_2})|101\rangle \\ &\quad +(-e^{-i(\theta_1+\theta_2)} - e^{i\theta_3})|110\rangle + (i - ie^{-i(\theta_1+\theta_2+\theta_3)})|111\rangle]. \end{aligned} \tag{20}$$

Second, we perform the joint projective-measurements to determine the required correlation functions $E(\theta_1, \theta_2, \theta_3)$ for various combinations of these local variables.

Experimentally, the above two steps can be repeated many times, and thus the correlation function can be determined by

$$E(\theta_1, \theta_2, \theta_3) = P_{111} + P_{100} + P_{010} + P_{001} - P_{011} - P_{101} - P_{110} - P_{000}. \tag{21}$$

Here, $\sum_{i,j,k=0,1} P_{ijk} = 1$ with P_{ijk} being the probability of the state $|\psi''_{\rm GHZ}\rangle$ collapsing to the joint basis $|ijk\rangle$. With these projective measurements, various correlation functions required can be measured and then the tripartite Mermin inequality (1) can be tested. Theoretically, the correlation function can be easily calculated as

$$E(\theta_1, E(\theta_1, \theta_2, \theta_3) = \langle \psi''_{\rm GHZ}|\hat{P}_T|\psi''_{\rm GHZ}\rangle = -\cos(\theta_1 + \theta_2 + \theta_3), \tag{22}$$

with the joint projective operator $\hat{P}_T = \sigma_{z_1} \otimes \sigma_{z_2} \otimes \sigma_{z_3} = |111\rangle\langle 111| + |100\rangle\langle 100| + |010\rangle\langle 010| + |001\rangle\langle 001| - |011\rangle\langle 011| - |101\rangle\langle 101| - |110\rangle\langle 110| - |000\rangle\langle 000|$. For the suitable choices of the local observables, e.g., $\{\theta_1, \theta_2, \theta_3, \theta'_1, \theta'_2, \theta'_3\} = \{0, \pi/4, \pi/2, \pi/4, \pi/4, \pi\}$, we have the ideal value of the Q-parameter in Eq. (1):

$$Q_i = \sqrt{2} + 1 > 2. \tag{23}$$

This indicates that the inequality (1), namely $Q_i \leq 2$, is violated. Furthermore, for the parameters $\{\theta_1, \theta_2, \theta_3, \theta'_1, \theta'_2, \theta'_3\} = \{\pi/4, 0, 0, 3\pi/4, \pi/2, \pi/2\}$, the above tripartite Mermin inequality is maximally violated, i.e., $Q_i = 2\sqrt{2}$.

In the usual tomographic reconstructions only one basis, e.g., $|ijk\rangle$, is collapsed for one kind of projective measurement $\hat{P}_{ijk} = |ijk\rangle\langle ijk|$. This implies that seven kinds of projective measurements are required to complete the above joint projection $\hat{P}_{ijk}$. However, by the spectral joint-measurements introduced in Refs. [40, 41], the probabilities $P_{ijk}(i, j, k = 0, 1)$ can be determined simultaneously by just the spectral measurements of the transmission through the driven cavity; each peak of the transmission spectra marks one of the basis $|ijk\rangle$, and its relative height refers to the relevant probability P_{ijk}. Specifically, for one set of classical variables $\{\theta_1, \theta_2, \theta_3, \theta'_1, \theta'_2, \theta'_3\} = \{0, \pi/4, \pi/2, \pi/4, \pi/4, \pi\}$, Figs. 2(a-d) show how the spectra of the driven cavity distribute (versus the qubit-driving detuning) for the state (20). For instance, four peaks, marking respectively the basis states $|000\rangle$, $|011\rangle$, $|101\rangle$, and $|110\rangle$, are shown in Fig. 2(a). Their relative heights are equivalent: $P_{000} = P_{011} = P_{101} = P_{110} = 0.25$. Thus, the correlation function between

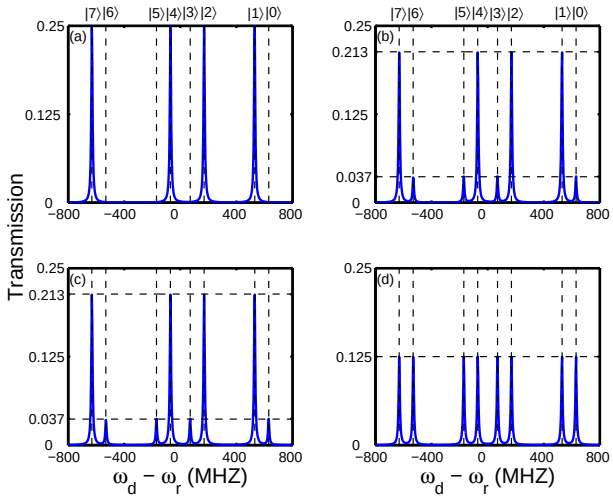

FIG. 2: (Color online) Transmission spectra of the driven cavity versus the detuning for the evolved state $|\psi''_{\rm GHZ}\rangle$ with the classical variables $\{\theta_1, \theta_2, \theta_3, \theta'_1, \theta'_2, \theta'_3\} = \{0, \pi/4, \pi/2, \pi/4, \pi/4, \pi\}$. Here, (a)-(d) correspond respectively to the parameters $\{\theta'_1, \theta_2, \theta_3\}$, $\{\theta_1, \theta'_2, \theta_3\}$, $\{\theta_1, \theta_2, \theta'_3\}$, and $\{\theta'_1, \theta'_2, \theta'_3\}$. With these spectral distributions, the correlation functions required for testing the Mermin inequality (1) can be calculated. Other parameters of the system are the same as those used in Fig. 1.

the three local variables can be easily calculated as

$$\begin{cases} E(\pi/4, 0, 0) = 1, \\ E(\pi/2, 0, 0) = 0.704, \\ E(\pi/4, \pi/2, 0) = 0.704, \\ E(\pi/2, \pi/2, 0) = 0. \end{cases}$$

Consequently, the numerical experimental result of the Q-parameter is

$$Q_e = 2.408 \approx \sqrt{2} + 1 > 2, \tag{24}$$

and thus the tripartite Mermin inequality is violated. Similarly, for another set of classical variables $\{\theta_1, \theta_2, \theta_3, \theta'_1, \theta'_2, \theta'_3\} = \{\pi/4, 0, 0, 3\pi/4, \pi/2, \pi/2\}$, Figs. 3(a-d) show all the probabilities of eight bases in the present three-qubit system. Again, the involved correlation functions are calculated as $(E(\theta'_1, \theta_2, \theta_3),\ E(\theta_1, \theta'_2, \theta_3),\ E(\theta_1, \theta_2, \theta'_3),\ E(\theta'_1, \theta'_2, \theta'_3))$=(0.704, 0.704, 0.704, -0.704). As a consequence,

$$Q_e = 2.816 \approx 2\sqrt{2} > 2, \tag{25}$$

and the Mermin inequality (1) is violated more strongly.

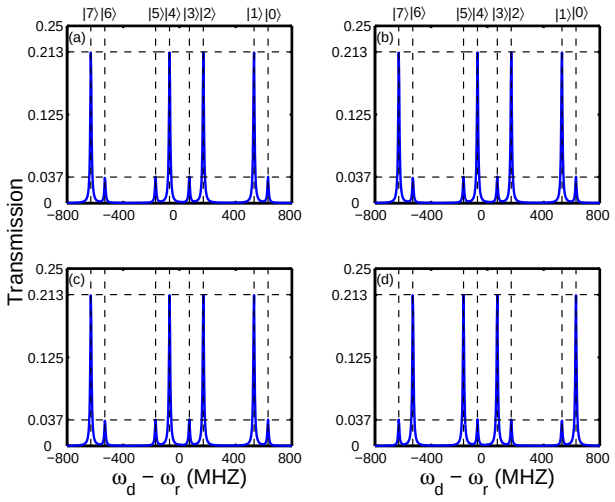

FIG. 3: (Color online) Transmission spectra of the driven cavity versus the qubit-drive detuning for the set of local variables $\{\theta_1, \theta_2, \theta_3, \theta_1', \theta_2', \theta_3'\} = \{\pi/4, 0, 0, 3\pi/4, \pi/2, \pi/2\}$. Other parameters are the same as those in Fig. 1.

IV. DISCUSSION

We have proposed a direct and experimentally-feasible scheme to test tripartite Mermin inequality with cavity-qubit system, wherein quantum state of three qubits without direct interbit couplings is detected by measuring the dispersively-coupled cavity spectra. We have numerically demonstrated that the local-variable-dependent probabilities of various bases superposed in the local-variable-encoded GHZ state can be directly read out by the cavity transmission. With these probabilities, various correlation functions on the local variables of individual qubits are easily calculated, and consequently the violations of the three-particle Mermin inequality are tested. Specifically, a few examples were utilized to numerically confirm the tests. Certainly, the present proposal could be generalized to test other Bell-type inequalities with more than three qubits in a straightforward way.

Note that in our numerical experiments little deviations exist between our estimated results and the ideal predictions. For example, if the local variables are set as $\{\theta_1, \theta_2, \theta_3, \theta_1', \theta_2', \theta_3'\} = \{0, \pi/4, \pi/2, \pi/4, \pi/4, \pi\}$, the values of Q-paramter given by our numerical experiments is $Q_e = 2.408$, which deviates the ideal values $Q_i = \sqrt{2} + 1$ with a quantity $\Delta Q = Q_i - Q_e = 0.006$. Also, for local variables $\{\theta_1, \theta_2, \theta_3, \theta_1', \theta_2', \theta_3'\} = \{\pi/4, 0, 0, 3\pi/4, \pi/2, \pi/2\}$ the inequality (1) should be maximally violated with $Q_i = 2\sqrt{2}$, but our numerical experiment yields $Q_e = 2.816 = Q_i - 0.012$. These deviations are due to the existence of the dissipation of the cavity, which yields

various finite widths of the transmission spectra through the driven cavity. As a consequence, the relative heights of the measured peaks are lower than those of the ideal δ-type peaks. As the measured values are less than those for the ideal cases, it is sufficient to show the violation of the Mermin inequality.

Acknowledgments

This work was supported in part by the National Science Foundation grant No. 10874142, 90921010, and the National Fundamental Research Program of China through Grant No. 2010CB92304, and the Fundamental Research Funds for the Central Universities No. SWJTU09CX078, and Centre for Quantum Technology, NRF (Singapore) grant number: WBS: R-710-000-008-271.

APPENDIX: TRANSMISSION OF A DRIVEN CAVITY

In this appendix, the transmission spectrum of a three-qubit in a driven cavity is calculated in detail. The transition frequencies of the three qubits are denoted as ω_1, ω_2 and ω_3, respectively. We assume that the dispersive condition

$$0 < \frac{g_j}{\Delta_j}, \frac{g_j g_{j'}}{\Delta_j \Delta_{jj'}}, \frac{g_j g_{j'}}{\Delta_{j'} \Delta_{jj'}} \ll 1, \ j \neq j' = 1, 2, 3, \tag{A1}$$

is satisfied for ensuring the effective dispersive coupling $\sigma_{z_j} \hat{a}^\dagger \hat{a}$ between the jth qubit and the cavity. These conditions also ensure that the interbit interactions are negligible. Also, $\Delta_j = \omega_j - \omega_r$ denotes the detuning between the jth qubit and the cavity, and $\Delta_{jj'} = \omega_j - \omega_j'$ the detuning between the jth and j'th qubits.

In a framework rotating at ω_d, the effective Hamiltonian of the qubit-cavity system is

$$\begin{aligned} \tilde{H} \ &= \ (-\delta + \Gamma_1 \sigma_{z_1} + \Gamma_2 \sigma_{z_2} + \Gamma_3 \sigma_{z_3}) \hat{a}^\dagger \hat{a} \\ &+ \ \frac{\tilde{\omega}_1}{2} \sigma_{z_1} + \frac{\tilde{\omega}_2}{2} \sigma_{z_2} + \frac{\tilde{\omega}_3}{2} \sigma_{z_3} + \epsilon (\hat{a}^\dagger + \hat{a}), \end{aligned} \tag{A2}$$

where $\Gamma_j = g_j^2 / \Delta_j$, $\tilde{\omega}_j = \omega_j + \Gamma_j$, $(j = 1, 2, 3)$, and $\delta = \omega_d - \omega_r$ is the detuning of the cavity from the driving. The master equation for the complete system reads

$$\dot{\varrho} \ = \ -i[\tilde{H}, \varrho] + \kappa (\hat{a} \varrho \hat{a}^\dagger - \hat{a}^\dagger \hat{a} \varrho / 2 - \varrho \hat{a}^\dagger \hat{a} / 2), \tag{A3}$$

where ϱ is the density matrix of the qubit-cavity system.

From the above master equation, the equations of motion for the mean values of various operators are

$$\frac{d\langle\hat{a}^\dagger\hat{a}\rangle}{dt} = -\kappa\langle\hat{a}^\dagger\hat{a}\rangle - 2\epsilon\mathrm{Im}\langle\hat{a}\rangle, \tag{A4a}$$

$$\begin{aligned}\frac{d\langle\hat{a}\rangle}{dt} &= (i\delta - \frac{\kappa}{2})\langle\hat{a}\rangle - i\epsilon \\ &- i\Gamma_1\langle\hat{a}\sigma_{z_1}\rangle - i\Gamma_2\langle\hat{a}\sigma_{z_2}\rangle - i\Gamma_3\langle\hat{a}\sigma_{z_3}\rangle,\end{aligned} \tag{A4b}$$

with

$$\begin{aligned}\frac{d\langle\hat{a}\sigma_{z_1}\rangle}{dt} &= (i\delta - \frac{\kappa}{2})\langle\hat{a}\sigma_{z_1}\rangle - i\epsilon\langle\sigma_{z_1}\rangle - i\Gamma_2\langle\hat{a}\sigma_{z_1}\sigma_{z_2}\rangle \\ &- i\Gamma_1\langle\hat{a}\rangle - i\Gamma_3\langle\hat{a}\sigma_{z_1}\sigma_{z_3}\rangle,\end{aligned} \tag{A4c}$$

$$\begin{aligned}\frac{d\langle\hat{a}\sigma_{z_2}\rangle}{dt} &= (i\delta - \frac{\kappa}{2})\langle\hat{a}\sigma_{z_2}\rangle - i\epsilon\langle\sigma_{z_2}\rangle - i\Gamma_1\langle\hat{a}\sigma_{z_2}\sigma_{z_1}\rangle \\ &- i\Gamma_2\langle\hat{a}\rangle - i\Gamma_3\langle\hat{a}\sigma_{z_2}\sigma_{z_3}\rangle,\end{aligned} \tag{A4d}$$

$$\begin{aligned}\frac{d\langle\hat{a}\sigma_{z_3}\rangle}{dt} &= (i\delta - \frac{\kappa}{2})\langle\hat{a}\sigma_{z_3}\rangle - i\epsilon\langle\sigma_{z_3}\rangle - i\Gamma_1\langle\hat{a}\sigma_{z_3}\sigma_{z_1}\rangle \\ &- i\Gamma_3\langle\hat{a}\rangle - i\Gamma_2\langle\hat{a}\sigma_{z_3}\sigma_{z_2}\rangle,\end{aligned} \tag{A4e}$$

and

$$\begin{aligned}\frac{d\langle\hat{a}\sigma_{z_1}\sigma_{z_2}\rangle}{dt} &= (i\delta - \frac{\kappa}{2})\langle\hat{a}\sigma_{z_1}\sigma_{z_2}\rangle - i\epsilon\langle\sigma_{z_1}\sigma_{z_2}\rangle \\ &- i\Gamma_1\langle\hat{a}\sigma_{z_2}\rangle - i\Gamma_2\langle\hat{a}\sigma_{z_1}\rangle \\ &- i\Gamma_3\langle\hat{a}\sigma_{z_1}\sigma_{z_2}\sigma_{z_3}\rangle,\end{aligned} \tag{A4f}$$

$$\begin{aligned}\frac{d\langle\hat{a}\sigma_{z_2}\sigma_{z_3}\rangle}{dt} &= (i\delta - \frac{\kappa}{2})\langle\hat{a}\sigma_{z_2}\sigma_{z_3}\rangle - i\epsilon\langle\sigma_{z_2}\sigma_{z_3}\rangle \\ &- i\Gamma_2\langle\hat{a}\sigma_{z_3}\rangle - i\Gamma_3\langle\hat{a}\sigma_{z_2}\rangle \\ &- i\Gamma_1\langle\hat{a}\sigma_{z_1}\sigma_{z_2}\sigma_{z_3}\rangle,\end{aligned} \tag{A4g}$$

$$\begin{aligned}\frac{d\langle\hat{a}\sigma_{z_1}\sigma_{z_3}\rangle}{dt} &= (i\delta - \frac{\kappa}{2})\langle\hat{a}\sigma_{z_1}\sigma_{z_3}\rangle - i\epsilon\langle\sigma_{z_1}\sigma_{z_3}\rangle \\ &- i\Gamma_1\langle\hat{a}\sigma_{z_3}\rangle - i\Gamma_3\langle\hat{a}\sigma_{z_1}\rangle \\ &- i\Gamma_2\langle\hat{a}\sigma_{z_1}\sigma_{z_2}\sigma_{z_3}\rangle,\end{aligned} \tag{A4h}$$

$$\begin{aligned}\frac{d\langle\hat{a}\sigma_{z_1}\sigma_{z_2}\sigma_{z_3}\rangle}{dt} &= (i\delta-\frac{\kappa}{2})\langle\hat{a}\sigma_{z_1}\sigma_{z_2}\sigma_{z_3}\rangle \\ &- i\epsilon\langle\sigma_{z_1}\sigma_{z_2}\sigma_{z_3}\rangle - i\Gamma_1\langle\hat{a}\sigma_{z_2}\sigma_{z_3}\rangle \\ &- i\Gamma_2\langle\hat{a}\sigma_{z_1}\sigma_{z_3}\rangle - i\Gamma_3\langle\hat{a}\sigma_{z_1}\sigma_{z_2}\rangle,\end{aligned} \tag{A4i}$$

$$\frac{d\langle\sigma_{z_1}\rangle}{dt} = \frac{d\langle\sigma_{z_2}\rangle}{dt} = \frac{d\langle\sigma_{z_3}\rangle}{dt} = 0, \tag{A4j}$$

$$\frac{d\langle\sigma_{z_1}\sigma_{z_2}\rangle}{dt} = \frac{d\langle\sigma_{z_1}\sigma_{z_3}\rangle}{dt} = \frac{d\langle\sigma_{z_2}\sigma_{z_3}\rangle}{dt} = 0, \tag{A4k}$$

$$\frac{d\langle\sigma_{z_1}\sigma_{z_2}\sigma_{z_3}\rangle}{dt} = 0, \tag{A4l}$$

The steady-state distribution of the intracavity photon number can be obtained by solving the Eqs. (A4 a-i) under the steady-state condition, i.e., all the derivatives in the left sides of above equations equate 0. Then, by numerical method, the steady-state average photons number inside the cavity can be obtained. Similar to the single-qubit and two-qubit cases in Ref. [40, 41], information of these eight basis states in arbitrary three-qubit state can be extracted from the spectra of the cavity transmission, since each peak marks one of the eight bases, and its relative height refers to its probability superposed in the measured three-qubit state.

---

[1] A. Einstein, B. Podolsky, and N. Rosen, Phys. Rev. **47**, 777 (1935)

[2] D. Bouwmeester, A. Ekert, and A. Zeilinger, *The Physics of Quantum Information* (Springer, Berlin, 2000)

[3] M. A. Nielsen and I. L. Chuang, *Quantum Computation and Quantum Information* (Cambridge University Press, Cambridge, England, 2000)

[4] C. H. Bennett, G. Brassard, C. Crépeau, R. Jozsa, A. Peres, and W. K. Wootters, Phys. Rev. Lett. **70**, 1895 (1993)

[5] D. Bouwmeester, J. W. Pan, K. Mattle, M. Eibl, H. Weinfurter, and A. Zeilinger, Nature (London) **390**, 575 (1997); D. Boschi, S. Branca, F. De Martini, L. Hardy, and S. Popescu, Phys. Rev. Lett. **80**, 1121 (1998)

[6] M. Hillery, V. Bužek, and A. Berthiaume, Phys. Rev. A **59**, 1829 (1999)

[7] M. A. Nielsen, Phys. Rev. Lett. **83**, 436 (1999)

[8] J. S. Bell, Physics **1**, 195 (1964)

[9] J. F. Clauser, M. A. Horne, A. Shimony, and R. A. Holt, Phys. Rev. Lett. **23**, 880 (1969)

[10] A. Aspect, J. Dalibard, and G. Roger, Phys. Rev. Lett. **49**, 1804 (1982); W. Tittel, J. Brendel, H. Zbinden, and N. Gisin, Phys. Rev. Lett. **81**, 3563 (1998); G. Weihs, T. Jennewein, C. Simon, H. Weinfurter and A. Zeilinger, Phys. Rev. Lett. **81**, 5039 (1998)

[11] M. A. Rowe, D. Kielpinski, V. Meyer, C. A. Sackett, W. M. Itano, C. Monroe, and D. J. Wineland, Nature (London) **409**, 791 (2001)

[12] D. N. Matsukevich, P. Maunz, D. L. Moehring, S. Olmschenk, and C. Monroe, Phys. Rev. Lett. **100**, 150404 (2008)

[13] Y. Hasegawa, R. Loidl, G. Badurek, M. Baron, and H. Rauch, Nature (London) **425**, 45 (2003)

[14] M. Ansmann, H. Wang, R. C. Bialczak, M. Hofheinz, E. Lucero, M. Neeley, A. D. O'Connell, D. Sank, M. Weides, J. Wenner, A. N. Cleland, J. M. Martinis, Nature (London) **461**, 504 (2009)

[15] L. F. Wei, Yu-xi Liu, and F. Nori, Phys. Rev. B **72**, 104516 (2005); L. F. Wei, Yu-xi Liu, M. J. Storcz, and F. Nori, Phys. Rev. A **73**, 052307 (2006)

[16] J. I. Cirac and P. Zoller, Phys. Rev. A **50**, R2799 (1994)

[17] A. Rauschenbeutel, G. Nogues, S. Osnaghi, P. Bertet, M. Brune, J. M. Raimond, S. Haroche, Science **288**, 2024 (2000)

[18] D. Bouwmeester, J. W. Pan, M. Daniell, H. Weinfurter, and A. Zeilinger, Phys. Rev. Lett. **82**, 1345 (1999)

[19] J. W. Pan, D. Bouwmeester, M. Daniell, H. Weinfurter and A. Zeilinger, Nature (London) **403**, 515 (2000)

[20] K. J. Resch, P. Walther, and A. Zeilinger, Phys. Rev. Lett. **94**, 070402 (2005)

[21] Z. Zhao, T. Yang, Y. A. Chen, A. N. Zhang, M. Żukowski and J. W. Pan, Phys. Rev. Lett. **91** 180401 (2003)

[22] Q. A. Turchette, C. S. Wood, B. E. King, C. J. Myatt, D. Leibfried, W. M. Itano, C. Monroe, and D. J. Wineland, Phys. Rev. Lett. **81**, 3631 (1998)

[23] C. A. Sackett, D. Kielpinski, B. E. King, C. Langer, V. Meyer, C. J. Myatt, M. Rowe, Q. A. Turchette, W. M. Itano, D. J. Wineland, and C. Monroe, Nature (London) **404**, 256 (2000)

[24] G. Kirchmair, F. Zähringer, R. Gerritsma, M. Kleinmann1, O. Gühne, A. Cabello, R. Blatt and C. F. Roos, Nature (London) **460** 494 (2009)

[25] F. Plastina, R. Fazio, and G. M. Palma, Phys. Rev. B **64**, 113306 (2001); J. Siewert and R. Fazio, Phys. Rev. Lett. **87**, 257905 (2001)

[26] L. F. Wei, Yu-xi Liu and Franco Nori, Phys. Rev. Lett. **96**, 246803 (2006)

[27] N. D. Mermin, Phys. Rev. Lett. **65**, 1838 (1990); M. Ardehali, Phys. Rev. A **46**, 5375 (1992); A. V. Belinskii and D. N. Klyshko, Phys. Usp. 36, 653 (1993)

[28] D. M. Greenberger, M. A. Horne, and A. Zeilinger, in *Bell's Theorem, Quantum Theory, and Conceptions of the Universe*, edited by M. Kafatos (Kluwer Academic, Dordrecht, 1989); D. M. Greenberger, M. A. Horne, A. Shimony, and A. Zeilinger, Am. J. Phys. **58**, 1131 (1990)

[29] M. Tavis and F. W. Cummings, Phys. Rev. **170**, 379 (1968)

[30] A. Blais, J. Gambetta, A. Wallraff, D. I. Schuster, S. M. Girvin, M. H. Devoret, and R. J. Schoelkopf, Phys. Rev. A **75**, 032329 (2007)

[31] C. W. Wu, Y. Han, H. Y. Li, Z. J. Deng, P. X. Chen, and C. Z. Li, Phys. Rev. A **82**, 014303 (2010)

[32] J. Wei and E. Norman, J. Math. Phys. **4**, 575 (1963)

[33] S. B. Zheng, Phys. Rev. A **66**, 060303(R) (2002)

[34] K. Mølmer and A. Sørensen, Phys. Rev. Lett. **82**, 1835 (1999)

[35] Y. D. Wang, S. Chesi, D. Loss, and C. Bruder, Phys. Rev. B **81**, 104524 (2010)

[36] C. F. Roos, M. Riebe, H. Häffner, W. Hänsel, J. Benhelm, G. P. T. Lancaster, C. Becher, F. S. Kaler and R. Blatt, Science **304**, 1478 (2004)

[37] Yu-xi Liu, L. F. Wei, and F. Nori, Europhys. Lett. **67**, 874 (2004); L. F. Wei, Yu-xi Liu, M. J. Storcz, and F. Nori, Phys. Rev. A **73**, 052307 (2006)

[38] M. Neeley, R. C. Bialczak, M. Lenander, E. Lucero, M. Mariantoni, A. D. OConnell, D. Sank, H. Wang, M. Weides, J. Wenner, Y. Yin, T. Yamamoto, A. N. Cleland and J. M. Martinis, Nature **467**, 570 (2010)

[39] L. DiCarlo, M. D. Reed, L. Sun, B. R. Johnson, J. M. Chow, J. M. Gambetta, L. Frunzio, S. M. Girvin, M. H. Devoret and R. J. Schoelkopf, Nature **467**, 574 (2010)

[40] L. F. Wei, J. S. Huang, X. L. Feng, Z. D. Wang and C. H. Oh, arXiv: 1005. 2470

[41] J. S. Huang, L. F. Wei, and C. H. Oh, Phys. Rev. A **83**, 032110 (2011)